
Toward Clinical Application of Resting-State Functional Magnetic Resonance Imaging to Dementia

8

Yousuke Ogata and Takashi Hanakawa

Abstract

Functional magnetic resonance imaging (fMRI) has been widely used to assess brain activity in many fields including cognitive neuroscience and clinical medicine. Typically, fMRI requires a participant to perform a task of the investigator's interest during MRI acquisition. In this chapter, we introduce an emerging variant of the fMRI technique, resting-state fMRI (rs-fMRI), or resting-state functional connectivity MRI (rsfcMRI), in which a participant is only required to lie quietly within an MRI scanner. That is, rs-fMRI/rsfcMRI does not impose a demanding task on a participant. This property is potentially advantageous for the application of rs-fMRI/rsfcMRI to patients with neuropsychiatric disorders, including dementia, who might have difficulty performing tasks. We discuss the potential of rs-fMRI/rsfcMRI for the diagnosis of dementia and for understanding the mechanism underlying its clinical symptoms, taking into consideration that rs-fMRI/rsfcMRI functional connectivity analysis is increasingly used to identify subtle brain network changes caused by the pathophysiology of dementia.

Keywords

Resting-state functional connectivity MRI • Functional MRI • Functional connectivity • Default mode network

Y. Ogata • T. Hanakawa (✉)

Department of Advanced Neuroimaging, Integrative Brain Imaging Center, National Center of Neurology and Psychiatry, 4-1-1 Ogawa-Higashi, Kodaira, Tokyo 187-8551, Japan
e-mail: hanakawa@ncnp.go.jp

© Springer Japan 2017

H. Matsuda et al. (eds.), *Neuroimaging Diagnosis for Alzheimer's Disease and Other Dementias*, DOI 10.1007/978-4-431-55133-1_8

173

8.1 Introduction

Functional magnetic resonance imaging (fMRI) has been widely used to assess brain activity in many fields including cognitive neuroscience and clinical medicine. Typically, fMRI requires a participant to perform a task of the investigator's interest during MRI acquisition. Here, we introduce an emerging variant of the fMRI technique, resting-state fMRI (rs-fMRI), or resting-state functional connectivity MRI (rsfMRI), in which a participant is only required to lie quietly within an MRI scanner. That is, rs-fMRI/rsfMRI does not impose a demanding task on a participant. This property is potentially advantageous to the application of rs-fMRI/rsfMRI to patients with neuropsychiatric disorders who might have difficulty performing tasks.

8.2 Principles of Functional MRI

Increases in local neuronal activity are associated with increases in regional blood flow [1]. This relationship is a consequence of a complex sequence of cellular, metabolic, and vascular processes, collectively called neurovascular coupling. In particular, changes in oxygenation, blood flow, and blood volume are called hemodynamic changes. Hemodynamic changes induced by local neuronal and synaptic activity result in changes in MRI signal intensity. One MRI sequence, T2*-weighted MRI, is sensitive to the inhomogeneity of magnetic fields, which can be induced by changes in paramagnetic deoxyhemoglobin and diamagnetic oxyhemoglobin within red blood cells. These changes in deoxyhemoglobin and oxyhemoglobin result from oxygen consumption, which is secondary to aerobic metabolism in producing adenosine triphosphate, supporting local neuronal and synaptic activity. This T2* MRI signal change using deoxyhemoglobin as an internal contrast medium has been called the "blood-oxygen level-dependent (BOLD) effect" [2].

More precisely, demands of aerobic metabolism result in oxygen extraction from oxyhemoglobin, producing deoxyhemoglobin. This should at least temporarily increase the concentration of deoxyhemoglobin, which would reduce magnetic inhomogeneity and shorten T2*. Currently, however, we usually observe the phenomenon that deoxyhemoglobin is rather diluted because of the excessive inflow of oxygenated arterial blood flow. Dilution of deoxygenated hemoglobin stabilizes the local magnetic field and prolongs T2*. This effect results in increases in T2* MRI signals, which are now widely used as a surrogate marker of neural/synaptic activity. The advantages of this BOLD MRI technique include noninvasive measurements of human brain functions with a superior spatial resolution and a fine temporal resolution over other noninvasive brain mapping methods.

Since BOLD fMRI has made the measurement of brain function possible, many researchers have succeeded in visualizing task-related brain activity by comparing BOLD signals across experimental conditions such as sensory stimulus presentation, cognitive or motor performance, and resting state. This conventional type of fMRI is called "task fMRI." The aim of a task fMRI is often the functional localization of a

brain function related to the task of interest. More recently, various analyses have been applied to clarify the relationship between the activities of remote brain regions, that is, the functional binding of brain areas and their modulation across conditions (functional/effective connectivity). For example, a functional connectivity analysis looks at the simple correlation of task-related activity between remote brain areas; a psychophysiological interaction analysis examines the modulation of inter-areal correlation (i.e., functional connectivity) by stimulus or task conditions; the Granger causality analysis analyzes the time series correlation of activity between brain regions; and dynamic causal modeling models the transmission and causation of distributed dynamic systems modulated by external or contextual inputs. Basically, these analyses have been used to clarify the magnitude differences in brain activity across task conditions (task-related activity), the correlation of task-related activity between remote brain areas (functional connectivity), or the modulation of functional connectivity by task conditions (effective connectivity). Although the application of these task-related fMRIs to healthy participants is relatively easy, it is often difficult to apply them to patients with psychiatric and neurological disorders, particularly because they are likely to have difficulty performing demanding cognitive or motor tasks.

8.3 Resting-State Functional (Connectivity) MRI

8.3.1 Principles of Resting-State Functional (Connectivity) MRI

Here, we introduce the emerging methodology of rs-fMRI/rsfcMRI, because this technique is expected to break the limit of conventional task fMRI and to greatly expand the possibilities of the clinical application of BOLD fMRI. rs-fMRI/rsfcMRI is made possible by just acquiring continuous BOLD contrast images at rest; participants do not need to perform a motor/cognitive task or to pay attention to a stimulus presentation. To assess functional connectivity, rs-fMRI/rsfcMRI extracts low-frequency fluctuations from the BOLD fMRI time series taken at rest and then identifies a set of brain regions that shows a correlation between the BOLD signal time course in those fluctuations. This interregional correlation of low-frequency fluctuations is thought to reflect the state of functional connectivity between remote brain regions. Hereafter, we first explore the theoretical and analytical background of rs-fMRI/rsfcMRI, and then outline the potential applicability of rs-fMRI/rsfcMRI to the diagnosis of dementia.

Biswal and colleagues were the first to introduce the concept of rs-fMRI/rsfcMRI [3]. They focused on the BOLD signal time series of the motor cortex in both hemispheres and showed a high correlation of signal fluctuations between the bilateral motor cortices. This correlation in signal fluctuations was particularly obvious in low-frequency domains in the range of 0.08–0.1 Hz. In addition, they explored regions showing the BOLD signal time course correlated with that of the left motor cortex and found activity almost identical to the activity during a bilateral finger-tapping task.

This report was an epoch-making study, which suggested that resting-state BOLD signals contained information about the network architecture between brain areas. However, skepticism about this claim existed because the low-frequency domains of the BOLD signal time course include various types of physiological noise caused by respiration and pulsation. It took a while until the concept of rs-fMRI/rsfcMRI was widely accepted, when later studies showed that functional connectivity information contained in low-frequency BOLD fluctuations was separable from those derived from physiological noise [4, 5].

8.3.2 Default Mode Network (DMN)

In cognitive task fMRI and positron emission tomography (PET) experiments, it has long been known that some brain areas show decreases of the BOLD signal/blood flow (i.e., deactivation), irrespective of the type of cognitive task. Such “universal deactivation” is often seen in the medial frontal area, medial and lateral parietal areas, and inferior temporal area. Conventionally, this phenomenon was thought to reflect redistribution of cerebral blood flow (i.e., intercerebral steal phenomenon) rather than a change in neural activity. Raichle et al. first claimed that these changes of blood flow did not result from the intercerebral steal phenomenon but from increases in neuronal activity in these regions during rest compared with during cognitive task performance [6]. They used PET imaging to measure the oxygen uptake rate, the ratio of oxygen metabolism, and the cerebral blood flow, in participants during a cognitive task and also at rest with the eyes closed. As a result, parts of the brain regions showed increases in the oxygen uptake rate during the task whereas the same regions showed a decrease in the oxygen uptake rate during the eyes-closed rest condition. Here, a decrease in the oxygen uptake rate indicates an increase in local neural activity, and its increase indicates a reduction in local neural activity. Hence, these findings meant that in the areas with increases in blood flow during the eyes-closed rest, neuronal activity was actually increased, arguing against the interpretation of the intercerebral steal phenomenon. From these results, Raichle et al. proposed the hypothesis that the brain areas activated at rest, such as the medial frontal area, medial and lateral parietal areas, and inferior temporal area, may represent the “default mode” of the brain. They coined the term of “default mode network (DMN)” corresponding to the network consisting of the areas above. Later discovery of the DMN as a part of the resting-state network (RSN) has led to the explosion of rs-fMRI/rsfcMRI research in the field. The encounter of the two originally independent concepts, the principle of rsfcMRI by Biswal and the DMN by Raichle, has provided a strong driving force to propel rsfcMRI research toward clinical applications of rs-fMRI/rsfcMRI to dementia.

In addition to the DMN, Beckmann and colleagues used rs-fMRI/rsfcMRI and identified various RSNs such as the medial and lateral visual networks, auditory network, sensory motor network, visuospatial network, executive control network, and left and right dorsal attention networks. Nodes in each RSN show an interregional correlation of the temporal dynamics of the BOLD signal, which is the reason why rsfcMRI is able to assess functional connectivity in those RSNs (Fig. 8.1) [4].

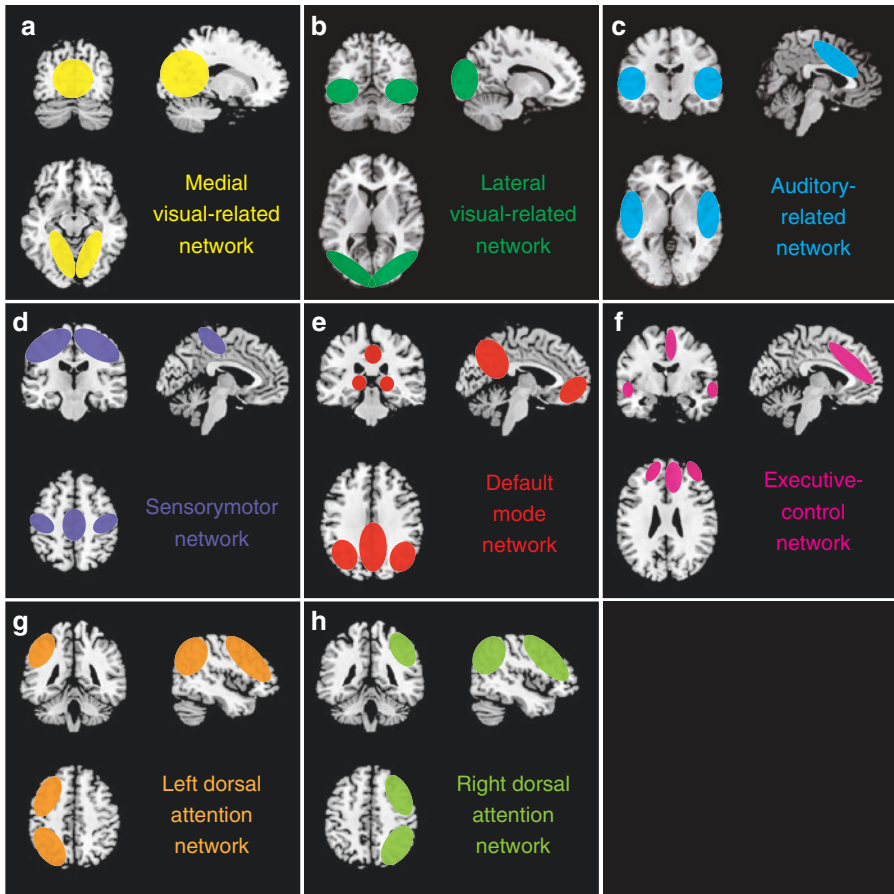


Fig. 8.1 Schema of resting-state networks. (a) medial visual-related network, (b) lateral visual-related network, (c) auditory-related network, (d) sensorimotor network, (e) default mode network, (f) executive control network, (g, h) left and right dorsal attention network

Because rsfMRI allows a noninvasive evaluation of those global brain network functions in healthy people and patients, many rsfMRI studies have been deployed in recent years.

8.3.3 Measurement of rs-fMRI/rsfMRI

The advantages of rs-fMRI/rsfMRI include user friendliness and ease of implementation. Experimenters do not have to design complex tasks or to set up a stimulus presentation and response recording systems. Participants do not have to exhaust themselves by working on difficult or nonsensical (at least to them) tasks. It is relatively easy to add rs-fMRI/rsfMRI to clinical routines of MRI examination as long as echo planar imaging (EPI) is available on the scanner.

To acquire EPIs for rs-fMRI/rsfcMRI, time to repetition (TR) is often set to about 2–3 s to cover the whole brain (Table 8.1). This temporal resolution is satisfactory for rs-fMRI/rsfcMRI because the chronological change of RSN BOLD signals primarily exists in a low-frequency domain ranging from ~0.08 to 0.1 Hz. To date, most rs-fMRI/rsfcMRI studies use a total acquisition time ranging from 5 to 10 min, corresponding to 150–300 EPI volumes. This is consistent with a previous report suggesting that the RSN can be reliably detected with assessment for several minutes [26]. In a large-scale cohort project on Alzheimer’s disease (AD) in the USA, the Alzheimer’s Disease Neuroimaging Initiative 2 (ADNI2), the rs-fMRI/rsfcMRI protocol uses a TR of 3 s, and a total acquisition time of 7 min (140 EPI volumes). For total acquisition time, however, Birn et al. [27] recently examined the test–retest reliability and similarity of RSNs across sessions. This study has shown that the reliability and similarity of functional connectivity can be improved by increasing the scan lengths from 5 min up to 13 min. However, this finding might

Table 8.1 Summary of the acquisition parameters in previous rsfcMRI studies

Author	Year	Subject	Static magnetic field (T)	Acquired volumes	TR (ms)	TE (ms)	Resolution (mm)
Jafri [7]	2008	Schizophrenia	3.0	168	1860	27	$3.75 \times 3.75 \times 4$
Vincent(Data1) [8]	2008	Healthy	3.0	110	3013	25	$4 \times 4 \times 4$
Vincent(Data2) [8]	2008	Healthy	3.0	66	5000	30	$2 \times 2 \times 2$
Vincent(Data3) [8]	2008	Healthy	3.0	76	5000	30	$2 \times 2 \times 2$
Uddin [9]	2009	Healthy	3.0	197	2000	25	$3 \times 3 \times 3$
Grigg [10]	2010	Healthy	3.0	170	2000	30	$3.125 \times 3.125 \times 5$
Sakoglu [11]	2010	Schizophrenia	3.0	249	1500	27	$3.75 \times 3.75 \times 4$
Allen [12]	2011	Healthy	3.0	152	2000	29	$3.75 \times 3.75 \times 4.55$
Arbabshirani [13]	2012	Healthy	3.0	200	1500	27	$3.75 \times 3.75 \times 4$
Bastin [14]	2012	Healthy	3.0	250	2130	40	$3.4 \times 3.4 \times 4$
Koch [15]	2012	MCI	3.0	120	3000	30	$3 \times 3 \times 4$
Li [16]	2013	AD	3.0	250	2000	30	$4 \times 4 \times 6$
Segall [17]	2012	Healthy	3.0	152	2000	29	$3.75 \times 3.75 \times 4.55$
Wang [18]	2012	Healthy	3.0	240	2000	31	$3.125 \times 3.125 \times 3.2$
Zuo [19]	2012	healthy	3.0	240	2000	27	$3.44 \times 3.44 \times 4$
Damoiseau [20]	2006	Healthy	1.5	200	2850	60	$3.3 \times 3.3 \times 3.3$
Wang [21]	2006	AD	1.5	170	2000	60	$3.75 \times 3.75 \times 7$
Sorg [22]	2007	MCI, AD	1.5	80	3000	50	$3.125 \times 3.125 \times 4.4$
Kelly [23]	2010	Healthy	1.5	180	2000	35	$3.5 \times 3.5 \times 5$
Adriaanse [24]	2012	AD	1.5	200	2850	60	$3.3 \times 3.3 \times 3.3$
Zarei [25]	2012	AD	1.5	200	2850	60	$3 \times 3 \times 3$

TR time to repetition, TE echo time, MCI mild cognitive impairment, AD Alzheimer’s disease

have resulted from both increases in scanning time and in the number of volumes. To test this, they assessed the effects of the total number of volumes by comparing results from two data sets with the same total scanning time but with a different number of EPI volumes. In practice, they excluded half the time points by sampling every second image from the first data set and created the half-volume second data set. The results showed that the benefit of increased reliability was found for the increase in the number of volumes as well as the increase in the length of time [27]. According to this result, it seems better to acquire as large a number of volumes as possible with a shortened TR. Currently, our group uses a 10-min scanning protocol with a TR of 2.5 s.

It is important to note that there are many possible states of “resting.” In rs-fMRI/rsfcMRI studies, a participant is usually instructed to stay relaxed in a comfortable position within a scanner, and not to think about anything particular or to imagine specific figures or scenes. However, a substantial variability exists across studies as to whether a participant is asked to close their eyes, open their eyes, or fixate on a visual target. However, there is a problem: the functional connectivity pattern may differ between the eyes-open condition and the eyes-closed condition [28]. To date, there is no rule of thumb to judge which condition is ideal for a particular rs-fMRI/rsfcMRI study. Yet one thing is certain: a single condition with either the eyes closed or the eyes open (with or without a fixation target) should be used consistently throughout a single study. In addition, some studies have suggested that RSNs, especially the visual network, may show variation related to the stage of sleep [29]. Currently, our group uses a visual fixation condition with the eyes open to prevent them from falling asleep completely and also to reduce head movement during scanning. This is because we believe that these factors should be controlled as much as possible to reduce possible confounding factors between individuals.

Moreover, a newly developed multimodal imaging technique has been applied for the simultaneous measurement of rs-fMRI/rsfcMRI with near-infrared spectroscopy or with the electroencephalogram [30].

8.3.4 Analysis of rs-fMRI/rsfcMRI

Many analytic methods have been proposed for rs-fMRI/rsfcMRI as they showcase the recent development of neuroimaging. rs-fMRI/rsfcMRI can be analyzed with software packages that have been used for the analysis of task-related fMRI such as statistical parametric mapping (<http://www.fil.ion.ucl.ac.uk/spm/doc/>), FSL (<http://fsl.fmrib.ox.ac.uk/fsl/fslwiki/>), and AFNI (<http://afni.nimh.nih.gov/afni/>), especially with implementation of extension programs such as the Data Processing Assistant for Resting-State fMRI (DPARSF; <http://rfmri.org/DPARSF>), the conn toolbox (<http://web.mit.edu/swg/software.htm> [31]), and the Group ICA of fMRI Toolbox (GIFT; <http://mialab.mrn.org/software/>).

An analysis method focusing on resting-state fluctuations of regional activity is called amplitude of low-frequency fluctuations (ALFF) or fractional ALFF (fALFF). ALFF is defined as the total power within the frequency range between 0.01 and

0.1 Hz in a given voxel; thus, ALFF retrieves local information about the amplitude of low-frequency fluctuations [32]. However, these low-frequency components often contain physiological noise resulting from respiration and pulsation. To overcome this limitation, Zuo and colleagues have proposed fALFF, which is calculated as the power of fluctuations within the low-frequency range (0.01–0.1 Hz) divided by the total power of fluctuations in the entire frequency range. Similar to ALFF, fALFF can index spontaneous brain activity within regions [33, 34]. For example, ALFF and fALFF can test whether two groups may differ in resting-state low-frequency fluctuations in each voxel or region of interest (ROI).

A majority of rs-fMRI/rsfMRI studies deal with functional connectivity. RsfMRI analyses explore the correlation of a low-frequency fluctuation of BOLD signals between regions. One of the simplest approaches is to test the correlation of low-frequency fluctuations of BOLD signals between a pair of ROIs. Another typical approach is a seed-to-voxel functional connectivity analysis, or seed-to-voxel analysis for short, adopted by Biswal and colleagues in their original paper [3]. By definition, a seed-to-voxel analysis uses an a priori ROI as the *seed region* and then tests the correlation of low-frequency fluctuations between the seed region and all other voxels in the brain. Seed-to-voxel analysis can explore all the voxels in the whole brain that have a significant correlational relationship with the seed region, yielding a functional connectivity map (Fig. 8.2). Because seed-to-voxel analysis is statistically straightforward and provides comprehensible results, it has become a popular technique. Despite the possibility of clear-cut results being provided, the technique has the major drawback of requiring a priori selection of a seed region. In other words, among the major techniques available for rs-fMRI/rsfMRI analysis, seed-based analysis is the most explicitly model-based or hypothesis-driven approach derived from traditional fMRI analysis. At the other extreme, independent component analysis (ICA) is a method for multivariate “exploratory” search in which a set of regions or networks having coherent BOLD signal fluctuations can be detected without an a priori model. ICA is a typical model-free analysis in contrast to the model-based functional connectivity analysis requiring an a priori ROI. ICA is originally a method developed for the estimation of a signal source or blind source separation; it is used to decompose an observed signal into a set of independent signal components, by hypothesizing that the observed signal is a linear sum of distinct components from different sources. In ICA of fMRI data, observed, spatially distributed time series BOLD signals are hypothesized as a linear mixture of spatially independent maps, each of which has certain temporal dynamics (signal time course). Thus, ICA of rsfMRI data identifies RSNs as spatially independent components and creates maps of RSNs accompanied with information about the temporal signal variations of each RSN (Fig. 8.3). An advantage of ICA is that it does not require a priori assumptions about the seed regions or functional connectivity networks. Further, ICA can separate signals that do not reflect neural activity: various types of noise resulting from body movement and physiological noise from respiration and pulsation typically seen in the white matter and cerebrospinal fluid space. Thus, ICA can be used as a filter to remove these noise components. Despite

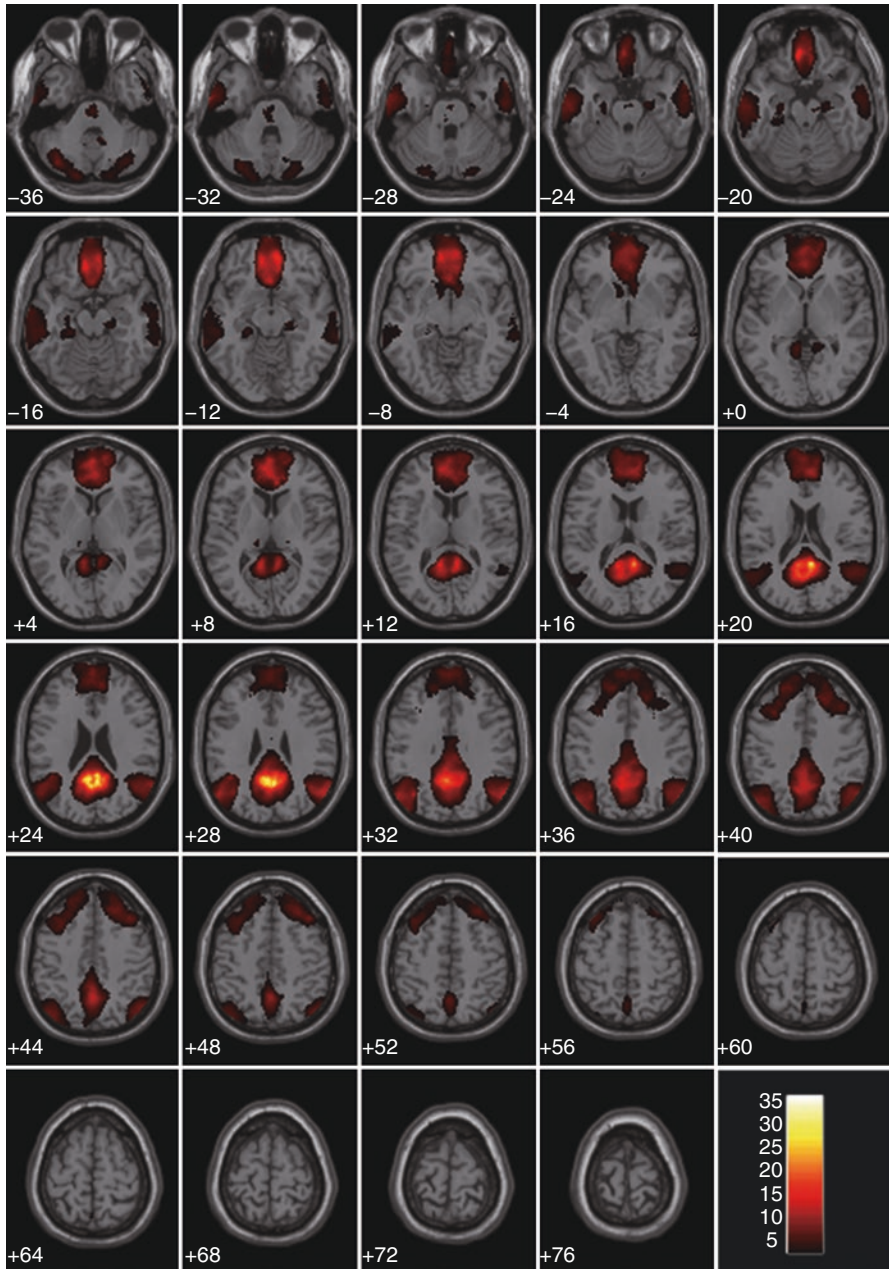


Fig. 8.2 Example of a seed-based analysis with seed ROI at the posterior cingulate cortex/precuneus in the healthy participants group. A significant correlation is observed in the medial part of the frontal lobe, lateral parietal lobe and the lateral inferior temporal gyrus as the default-mode network. The color bar indicates the correlation coefficient

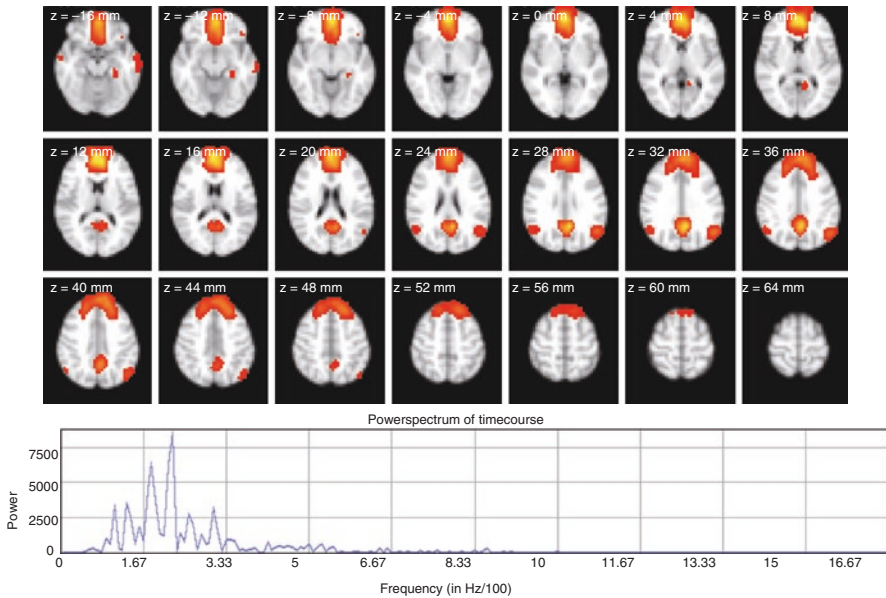


Fig. 8.3 Example of a default mode network identified by an independent component analysis. Because the peak of the power spectrum is observed from 0.02 to 0.03 Hz, we can interpret that this BOLD signal time course has low-frequency oscillation

these merits, a substantial challenge in ICA analysis resides in how to interpret the decomposed ICA components, because ICA-derived spatial maps do not have inherent physiological meanings. Traditionally, the interpretation rested completely upon researchers' eyes classifying the components into valuable and garbage. In this regard, frequency power analysis of the time course of ICA components often helps, because physiologically meaningful RSNs should have a frequency component between 0.08 and 0.1 Hz. For example, the component including most of the frequency-spectrum power above 0.1 Hz shows a “spotty” noise pattern with small clusters of voxels diffusely spread over the brain or ventricle [23]. Also, head motion-related ICA maps typically show a spike-like rapid change of time course. Therefore, motion-related ICA components are predominantly in a high-frequency range of the spectrum. More recently, a template matching method has been employed to match an ICA component from individuals to a single set of component maps representing typical RSNs [35].

Multivariate pattern analysis (MVPA) has significantly progressed the analysis of neuroimaging data in various ways. MVPA first selects a set of brain activity from multiple voxels or a correlation matrix derived from multiple pairs of ROIs, assuming that the selected multivariate data set (“a feature”) best characterizes a class or a label of interest. In the case of rsfMRI, a feature from each individual is typically a correlation matrix derived from several ROIs or from an extensive ROI set covering the entire brain (e.g., automated anatomical labeling); a class may be defined at a level of stimulus (e.g., an orientation of a line), task condition

(e.g., movement A or B), or population (diseased or healthy). A pattern discriminant algorithm is then applied to the correlation matrices to find a hyperplane or criteria that can best discriminate categories within the class. A discriminant algorithm, or a classifier, is often implemented by a form of supervised machine learning such as a support vector machine. After the classifier learns the criteria that best separates a multivariate pattern according to the input data, the capabilities of the classifier might be tested by applying it to a new functional connectivity data set. MVPA is expected to contribute to assisting in clinical diagnosis, provided that it can obtain high classification accuracy. Currently, rsfMRI-based MVPA classification typically achieves accuracy of about 60–80% (50% chance level) [7, 36, 37]; further improvement would be required for really helpful clinical utility.

Graph theory is one of the most recent network analysis methods and has been introduced to rsfMRI analysis. Graph theory analysis assumes functional connectivity as a “graph” that consists of a set of objects (“node”) corresponding to ROIs and directed or nondirected links (“edge”) connecting the objects. A graph characterizes the relationship or state of binding between nodes, namely, brain regions in the case of rsfMRI analysis. Graph theory analysis provides useful summary information about otherwise complicated relationships between multiple nodes: the small-worldness, the modularity, and the transmission efficiency. Furthermore, graph theory is used to decode the interaction between functional connectivity networks [38].

It is also important to develop analytic methods for multimodal recordings of resting-state brain activity. For example, Omata and colleagues used empirical mode decomposition to classify temporal dynamics of electroencephalogram alpha oscillations at rest into different patterns and then associated each component with rs-fMRI data [30].

8.3.5 rsfMRI for Diagnosis of Dementia

Recently, abnormal functional connectivity has been reported in various neuropsychiatric diseases such as schizophrenia, depression, and dementia. Particularly, a number of rs-fMRI/rsfMRI studies have been conducted in AD.

Greicius and colleagues first applied rsfMRI combined with ICA to AD and healthy control groups. They identified the spatial pattern of the DMN with ICA and then retrieved the BOLD signal time course from the DMN. Then, they performed a correlation analysis of the signal time series typical of the DMN with each individual’s rsfMRI data. As a result, AD patients showed a weak correlation with the typical DMN fluctuation pattern in the posterior cingulate cortex, the hippocampus, and the entorhinal cortex. This finding suggested that, in comparison with healthy participants, patients with AD had reduced functional connectivity in the DMN and medial temporal regions, which play an important role in the process of episodic memory [39]. This seminal report has shown that rs-fMRI/rsfMRI has the potential to provide a useful biomarker for detecting network abnormalities signifying dementia.

Since then, many studies have followed the study by Greicius and colleagues and have tested the feasibility of rs-fMRI/rsfMRI in the clinical diagnosis of

neuropsychiatric disorders. Many are interested in network abnormalities of the DMN as a hallmark of AD. As described above, the DMN is one of the RSNs and comprises the medial prefrontal area, posterior cingulate cortex-medial parietal area (precuneus), and the lateral parietal area, in which neural activity is higher at rest than during task engagement. AD transgenic mice show abnormal connectivity in the murine DMN including the human homologs of the posterior cingulate cortex/precuneus to the retrosplenial cortex after age-related deposition of beta-amyloid [40]. Additionally, patients with AD show abnormal functional connectivity of the hippocampus with important hubs of the DMN including the medial prefrontal cortex-ventral anterior cingulate cortex and the posterior cingulate cortex [21]. Zhang and colleagues classified patients with AD into mild, moderate, and severe groups according to the Clinical Dementia Rating (CDR) and the Mini-Mental State Examination (MMSE). When they performed seed-based rsfMRI analysis using the posterior cingulate cortex as a seed, patients with more severe AD showed a greater reduction in DMN connectivity between the medial prefrontal cortex and the posterior cingulate cortex [41].

Evidence indicates that AD patients may also have abnormal connectivity in other RSNs and also across different RSNs. Patients with amnesic mild cognitive impairment, probably a prodromal phase of AD, show decreased connectivity in the DMN, the hippocampus-posterior cingulate network, and also the attentional network [22]. Brier and colleagues performed seed-based analysis of rs-fMRI/rsfMRI in a cohort of 510 cases subdivided into normal (CDR of 0), very mild AD (CDR of 0–0.5), and mild AD. They analyzed not only the DMN but also the dorsal attention RSN, executive control RSN, salience RSN, and sensorimotor RSN. The results revealed abnormal intra-RSN connectivity as well as reduced across-RSN connectivity inversely correlated with CDR [42]. Zarei and colleagues classified the hippocampus into three subregions (head, body, and tail) according to its functional connectivity to other brain areas. The head, body, and tail of the hippocampus were strongly connected with the prefrontal cortex, posterior cingulate cortex, and thalamus, respectively. Then, they performed seed-based analysis to compare the connectivity of those hippocampal subnetworks between patients with AD and healthy older patients. The results revealed that there was a correlation between patients with AD who had increased prefrontal-hippocampal head connectivity and reduced posterior cingulate-hippocampal body connectivity and changes in MMSE scores [25, 42].

A famous biomarker of AD is the deposition of beta-amyloid in the brain, and such amyloid deposition can be detected with PET imaging. Interestingly, the posterior cingulate cortex and precuneus, hubs of the DMN, often show the deposition of beta-amyloid with PET imaging. The deposition of beta-amyloid does not always mean cognitive decline. For instance, task-related fMRI activity during a memory task is normal in older participants with amyloid deposition but with normal memory functions [43]. This finding indicates that AD is characterized by abnormal connectivity between the DMN and mesial temporal memory network in addition to the deposition of beta-amyloid. Put differently, the detection of both beta amyloid deposition and DMN abnormality may serve as a specific biomarker of AD. It is then tempting to test whether rs-fMRI/rsfMRI combined with amyloid PET may provide a better biomarker of predicting AD than the one provided by each technique alone.

In fact, rs-fMRI/rsfcMRI has been applied to cognitively normal or very mildly impaired pre-clinical AD as judged by amyloid PET [44]. Hedden and colleagues prescribed both rs-fMRI/rsfcMRI and PET with Pittsburgh compound B for older participants without clear cognitive decline. Participants with amyloid deposition had decreased DMN connectivity between the medial prefrontal cortex and posterior cingulate cortex and also between bilateral lateral parietal areas as compared with participants without amyloid deposition [43]. Consistent with this, Sheline and coworkers found that older people without cognitive decline had reduced connectivity of the posterior cingulate cortex with the hippocampus, parahippocampus, primary visual areas, and anterior cingulate cortex where amyloid deposition was identified [45]. Oh and colleagues took this one step further [46]. They used gray matter volumetric analysis of structural MRI in combination with amyloid PET and rs-fMRI/rsfcMRI. First, the analysis revealed that in the older population, increased amyloid deposition was correlated with the reduction in gray matter volume in the left inferior frontal gyrus. Second, the reduction of the gray matter volume of the posterior cingulate cortex was exclusively observed in participants with amyloid deposition there. Third, seed-based analysis of rsfcMRI showed that the left inferior frontal gyrus and the posterior cingulate cortex belonged to different RSNs. Last, abnormality of the left inferior frontal RNS was correlated with a reduction in working memory performance, whereas that of the posterior cingulate RNS was not. Taken together, a comprehensive workup with amyloid PET, structural MRI, and rs-fMRI/rsfcMRI likely provides invaluable information about the pathophysiology of preclinical AD.

As discussed, rsfcMRI is expected to assist in the clinical diagnosis of neuropsychiatric disorders. This may be achieved by combining multivariate information from rsfcMRI and pattern classification algorithms such as support vector machine to find a subtle difference between individuals. Such an approach is especially important in neuropsychiatric disorders without established biomarkers for a definite diagnosis such as mood disorders [37], schizophrenia [36], and autism [47]. Furthermore, Koch and coworkers have indicated the feasibility of rsfcMRI for the diagnosis of AD. They retrieved a seed (posterior cingulate cortex)-based feature and also an ICA-based feature from rsfcMRI data, and attempted to classify between AD and healthy older participants. They compared classification performance among the seed-based feature, ICA-based feature, and the combined seed- and ICA-based feature. The classification performance was 64% and 71% when they were based on either the seed- or ICA-based feature, respectively; however, the combined seed- and ICA-based feature achieved a classification performance of 97% [15]. This study has hinted on the usefulness of an rsfcMRI-based classification for the diagnosis of AD. Nevertheless, Koch and coworkers also reported that they were not able to classify between participants with and those without the ApoE4 allele, a risk factor of AD, suggesting a limitation of the current method [15].

We have argued for the feasibility of rs-fMRI/rsfcMRI for assisting in the early diagnosis of AD. It does not seem too difficult to implement rs-fMRI/rsfcMRI into clinical practice because of the convenience of the technique and the low burden to both patients and clinical practitioners. In combination with large imaging data projects such as ADNI, we foresee an explosion of rs-fMRI/rsfcMRI research and the clinical application of rs-fMRI/rsfcMRI to dementia.

References

1. Roy CS, Sherrington CS. On the regulation of the blood-supply of the brain. *J Physiol.* 1890;11(1-2):85-108.
2. Ogawa S, Lee TM, Kay AR, Tank DW. Brain magnetic resonance imaging with contrast dependent on blood oxygenation. *Proc Natl Acad Sci U S A.* 1990;87(24):9868-72.
3. Biswal B, Yetkin FZ, Haughton VM, Hyde JS. Functional connectivity in the motor cortex of resting human brain using echo-planar MRI. *Magn Reson Med.* 1995;34(4):537-41.
4. Beckmann CF, DeLuca M, Devlin JT, Smith SM. Investigations into resting-state connectivity using independent component analysis. *Philos Trans R Soc B-Biol Sci.* 2005;360(1457):1001-13. doi:10.1098/rstb.2005.1634.
5. Birn RM, Murphy K, Bandettini PA. The effect of respiration variations on independent component analysis results of resting state functional connectivity. *Hum Brain Mapp.* 2008;29(7):740-50. doi:10.1002/hbm.20577.
6. Raichle ME, MacLeod AM, Snyder AZ, Powers WJ, Gusnard DA, Shulman GL. A default mode of brain function. *Proc Natl Acad Sci U S A.* 2001;98(2):676-82.
7. Jafri MJ, Calhoun VD. Functional classification of schizophrenia using feed forward neural networks. *Conf Proc IEEE Eng Med Biol Soc.* 2006;(Suppl):6631-4.
8. Vincent JL, Kahn I, Snyder AZ, Raichle ME, Buckner RL. Evidence for a frontoparietal control system revealed by intrinsic functional connectivity. *J Neurophysiol.* 2008;100(6):3328-42. doi:10.1152/jn.90355.2008.
9. Uddin LQ, Kelly AMC, Biswal BB, Castellanos FX, Milham MP. Functional connectivity of default mode network components: correlation, anticorrelation, and causality. *Hum Brain Mapp.* 2009;30(2):625-37. doi:10.1002/hbm.20531.
10. Grigg O, Grady CL. The default network and processing of personally relevant information: converging evidence from task-related modulations and functional connectivity. *Neuropsychologia.* 2010;48(13):3815-23. doi:10.1016/j.neuropsychologia.2010.09.007.
11. Sakoglu U, Pearlson GD, Kiehl KA, Wang YM, Michael AM, Calhoun VD. A method for evaluating dynamic functional network connectivity and task-modulation: application to schizophrenia. *MAGMA.* 2010;23(5-6):351-66. doi:10.1007/s10334-010-0197-8.
12. Allen EA, Erhardt EB, Damaraju E, Gruner W, Segall JM, Silva RF, Havlicek M, Rachakonda S, Fries J, Kalyanam R, Michael AM, Caprihan A, Turner JA, Eichele T, Adelsheim S, Bryan AD, Bustillo J, Clark VP, Feldstein Ewing SW, Filbey F, Ford CC, Hutchison K, Jung RE, Kiehl KA, Kodituwakku P, Komesu YM, Mayer AR, Pearlson GD, Phillips JP, Sadek JR, Stevens M, Teuscher U, Thoma RJ, Calhoun VD. A baseline for the multivariate comparison of resting-state networks. *Front Syst Neurosci.* 2011;5:2. doi:10.3389/fnsys.2011.00002.
13. Arbabshirani MR, Havlicek M, Kiehl KA, Pearlson GD, Calhoun VD. Functional network connectivity during rest and task conditions: a comparative study. *Hum Brain Mapp.* 2012;34(11):2959-71. doi:10.1002/hbm.22118.
14. Bastin C, Yakushev I, Bahri MA, Fellgiebel A, Eustache F, Landeau B, Scheurich A, Feyers D, Collette F, Chetelat G, Salmon E. Cognitive reserve impacts on inter-individual variability in resting-state cerebral metabolism in normal aging. *NeuroImage.* 2012;63(2):713-22. doi:10.1016/j.neuroimage.2012.06.074.
15. Koch W, Teipel S, Mueller S, Benninghoff J, Wagner M, Bokde ALW, Hampel H, Coates U, Reiser M, Meindl T. Diagnostic power of default mode network resting state fMRI in the detection of Alzheimer's disease. *Neurobiol Aging.* 2012;33(3):466-78. doi:10.1016/j.neurobiolaging.2010.04.013.
16. Li R, Wu X, Chen K, Fleisher AS, Reiman EM, Yao L. Alterations of directional connectivity among resting-state networks in Alzheimer disease. *AJNR Am J Neuroradiol.* 2013;34(2):340-5. doi:10.3174/ajnr.A3197.
17. Segall JM, Allen EA, Jung RE, Erhardt EB, Arja SK, Kiehl K, Calhoun VD. Correspondence between structure and function in the human brain at rest. *Front Neuroinform.* 2012;6:10. doi:10.3389/fninf.2012.00010.

18. Wang Z, Liu J, Zhong N, Qin Y, Zhou H, Li K. Changes in the brain intrinsic organization in both on-task state and post-task resting state. *NeuroImage*. 2012;62(1):394–407. doi:[10.1016/j.neuroimage.2012.04.051](https://doi.org/10.1016/j.neuroimage.2012.04.051).
19. Zou Q, Ross TJ, Gu H, Geng X, Zuo XN, Hong LE, Gao JH, Stein EA, Zang YF, Yang Y. Intrinsic resting-state activity predicts working memory brain activation and behavioral performance. *Hum Brain Mapp*. 2013;34(12):3204–15. doi:[10.1002/hbm.22136](https://doi.org/10.1002/hbm.22136).
20. Damoiseaux JS, Rombouts S, Barkhof F, Scheltens P, Stam CJ, Smith SM, Beckmann CF. Consistent resting-state networks across healthy subjects. *Proc Natl Acad Sci U S A*. 2006;103(37):13848–53. doi:[10.1073/pnas.0601417103](https://doi.org/10.1073/pnas.0601417103).
21. Wang L, Zang Y, He Y, Liang M, Zhang X, Tian L, Wu T, Jiang T, Li K. Changes in hippocampal connectivity in the early stages of Alzheimer's disease: evidence from resting state fMRI. *NeuroImage*. 2006;31(2):496–504. doi:[10.1016/j.neuroimage.2005.12.033](https://doi.org/10.1016/j.neuroimage.2005.12.033).
22. Sorg C, Riedl V, Muehlau M, Calhoun VD, Eichele T, Laer L, Drzezga A, Foerstl H, Kurz A, Zimmer C, Wohlschlaeger AM. Selective changes of resting-state networks in individuals at risk for Alzheimer's disease. *Proc Natl Acad Sci U S A*. 2007;104(47):18760–5. doi:[10.1073/pnas.0708803104](https://doi.org/10.1073/pnas.0708803104).
23. Kelly RE, Alexopoulos GS, Wang ZS, Gunning FM, Murphy CF, Morimoto SS, Kanellopoulos D, Jia ZR, Lim KO, Hoptman MJ. Visual inspection of independent components: defining a procedure for artifact removal from fMRI data. *J Neurosci Methods*. 2010;189(2):233–45. doi:[10.1016/j.jneumeth.2010.03.028](https://doi.org/10.1016/j.jneumeth.2010.03.028).
24. Adriaanse SM, Sanz-Arigitia EJ, Binnewijzend MA, Ossenkuppe R, Tolboom N, van Assema DM, Wink AM, Boellaard R, Yaqub M, Windhorst AD. Amyloid and its association with default network integrity in Alzheimer's disease. *Hum Brain Mapp*. 2012;35(3):779–91.
25. Zarei M, Beckmann CF, Binnewijzend MA, Schoonheim MM, Oghabian MA, Sanz-Arigitia EJ, Scheltens P, Matthews PM, Barkhof F. Functional segmentation of the hippocampus in the healthy human brain and in Alzheimer's disease. *NeuroImage*. 2012;66:28–35.
26. Van Dijk KRA, Hedden T, Venkataraman A, Evans KC, Lazar SW, Buckner RL. Intrinsic functional connectivity as a tool for human connectomics: theory, properties, and optimization. *J Neurophysiol*. 2010;103(1):297–321. doi:[10.1152/jn.00783.2009](https://doi.org/10.1152/jn.00783.2009).
27. Birn RM, Molloy EK, Patriat R, Parker T, Meier TB, Kirk GR, Nair VA, Meyerand ME, Prabhakaran V. The effect of scan length on the reliability of resting-state fMRI connectivity estimates. *NeuroImage*. 2013;83:550–8. doi:[10.1016/j.neuroimage.2013.05.099](https://doi.org/10.1016/j.neuroimage.2013.05.099).
28. Patriat R, Molloy EK, Meier TB, Kirk GR, Nair VA, Meyerand ME, Prabhakaran V, Birn RM. The effect of resting condition on resting-state fMRI reliability and consistency: a comparison between resting with eyes open, closed, and fixated. *NeuroImage*. 2013;78:463–73. doi:[10.1016/j.neuroimage.2013.04.013](https://doi.org/10.1016/j.neuroimage.2013.04.013).
29. Samann PG, Wehrle R, Hoehn D, Spoormaker VI, Peters H, Tully C, Holsboer F, Czisch M. Development of the brain's default mode network from wakefulness to slow wave sleep. *Cereb Cortex*. 2011;21(9):2082–93. doi:[10.1093/cercor/bhq295](https://doi.org/10.1093/cercor/bhq295).
30. Omata K, Hanakawa T, Morimoto M, Honda M. Spontaneous slow fluctuation of EEG alpha rhythm reflects activity in deep-brain structures: a simultaneous EEG-fMRI study. *PLoS One*. 2013;8(6):12. doi:[10.1371/journal.pone.0066869](https://doi.org/10.1371/journal.pone.0066869).
31. Whitfield-Gabrieli S, Nieto-Castanon A. Conn: a functional connectivity toolbox for correlated and anticorrelated brain networks. *Brain Connect*. 2012;2(3):125–41. doi:[10.1089/brain.2012.0073](https://doi.org/10.1089/brain.2012.0073).
32. Zang Y-F, He Y, Zhu C-Z, Cao Q-J, Sui M-Q, Liang M, Tian L-X, Jiang T-Z, Wang Y-F. Altered baseline brain activity in children with ADHD revealed by resting-state functional MRI. *Brain and Development*. 2007;29(2):83–91. doi:[10.1016/j.braindev.2006.07.002](https://doi.org/10.1016/j.braindev.2006.07.002).
33. Yan CG, Liu DQ, He Y, Zou QH, Zhu CZ, Zuo XN, Long XY, Zang YF. Spontaneous brain activity in the default mode network is sensitive to different resting-state conditions with limited cognitive load. *PLoS One*. 2009;4(5):11. doi:[10.1371/journal.pone.0005743](https://doi.org/10.1371/journal.pone.0005743).
34. Zou Q-H, Zhu C-Z, Yang Y, Zuo X-N, Long X-Y, Cao Q-J, Wang Y-F, Zang Y-F. An improved approach to detection of amplitude of low-frequency fluctuation (ALFF) for resting-

- state fMRI: fractional ALFF. *J Neurosci Methods*. 2008;172(1):137–41. doi:[10.1016/j.jneumeth.2008.04.012](https://doi.org/10.1016/j.jneumeth.2008.04.012).
35. Salimi-Khorshidi G, Douaud G, Beckmann CF, Glasser MF, Griffanti L, Smith SM. Automatic denoising of functional MM data: combining independent component analysis and hierarchical fusion of classifiers. *NeuroImage*. 2014;90:449–68. doi:[10.1016/j.neuroimage.2013.11.046](https://doi.org/10.1016/j.neuroimage.2013.11.046).
 36. Arbabshirani MR, Kiehl KA, Pearson GD, Calhoun VD. Classification of schizophrenia patients based on resting-state functional network connectivity. *Front Neurosci*. 2013;7:16. doi:[10.3389/fnins.2013.00133](https://doi.org/10.3389/fnins.2013.00133).
 37. Craddock RC, Holtzheimer PE III, Hu XP, Mayberg HS. Disease state prediction from resting state functional connectivity. *Magn Reson Med*. 2009;62(6):1619–28. doi:[10.1002/mrm.22159](https://doi.org/10.1002/mrm.22159).
 38. Supekar K, Menon V, Rubin D, Musen M, Greicius MD. Network analysis of intrinsic functional brain connectivity in Alzheimer's disease. *PLoS Comput Biol*. 2008;4(6):11. doi:[10.1371/journal.pcbi.1000100](https://doi.org/10.1371/journal.pcbi.1000100).
 39. Greicius MD, Srivastava G, Reiss AL, Menon V. Default-mode network activity distinguishes Alzheimer's disease from healthy aging: evidence from functional MRI. *Proc Natl Acad Sci U S A*. 2004;101(13):4637–42. doi:[10.1073/pnas.0308627101](https://doi.org/10.1073/pnas.0308627101).
 40. Bero AW, Bauer AQ, Stewart FR, White BR, Cirrito JR, Raichle ME, Culver JP, Holtzman DM. Bidirectional relationship between functional connectivity and amyloid-beta deposition in mouse brain. *J Neurosci*. 2012;32(13):4334–40. doi:[10.1523/Jneurosci.5845-11.2012](https://doi.org/10.1523/Jneurosci.5845-11.2012).
 41. Zhang H-Y, Wang S-J, Liu B, Ma Z-L, Yang M, Zhang Z-J, Teng G-J. Resting brain connectivity: changes during the progress of alzheimer disease. *Radiology*. 2010;256(2):598–606.
 42. Brier MR, Thomas JB, Snyder AZ, Benzinger TL, Zhang D, Raichle ME, Holtzman DM, Morris JC, Ances BM. Loss of intranetwork and internetwork resting state functional connections with Alzheimer's disease progression. *J Neurosci*. 2012;32(26):8890–9. doi:[10.1523/Jneurosci.5698-11.2012](https://doi.org/10.1523/Jneurosci.5698-11.2012).
 43. Sperling RA, LaViolette PS, O'Keefe K, O'Brien J, Rentz DM, Pihlajamaki M, Marshall G, Hyman BT, Selkoe DJ, Hedden T. Amyloid deposition is associated with impaired default network function in older persons without dementia. *Neuron*. 2009;63(2):178.
 44. Sheline YI, Raichle ME. Resting state functional connectivity in preclinical Alzheimer's disease. *Biol Psychiatry*. 2013;74(5):340–7. doi:[10.1016/J.Biopsych.2012.11.028](https://doi.org/10.1016/J.Biopsych.2012.11.028).
 45. Sheline YI, Raichle ME, Snyder AZ, Morris JC, Head D, Wang SZ, Mintun MA. Amyloid plaques disrupt resting state default mode network connectivity in cognitively normal elderly. *Biol Psychiatry*. 2010;67(6):584–7. doi:[10.1016/J.Biopsych.2009.08.024](https://doi.org/10.1016/J.Biopsych.2009.08.024).
 46. Oh H, Mormino EC, Madison C, Hayenga A, Smiljic A, Jagust WJ. Beta-amyloid affects frontal and posterior brain networks in normal aging. *NeuroImage*. 2011;54(3):1887–95. doi:[10.1016/j.neuroimage.2010.10.027](https://doi.org/10.1016/j.neuroimage.2010.10.027).
 47. Iidaka T. Resting state functional magnetic resonance imaging and neural network classified autism and control. *Cortex*. 2015;63:55–67. doi:[10.1016/j.cortex.2014.08.011](https://doi.org/10.1016/j.cortex.2014.08.011).